Metal-Induced Structural Organization and Stabilization of the Metalloregulatory Protein MntR†

Misha V. Golynskiy,‡ Talib C. Davis,‡ John D. Helmann,§ and Seth M. Cohen*,‡

Department of Chemistry and Biochemistry, University of California, San Diego, La Jolla, California 92093-0358, and Department of Microbiology, Wing Hall, Cornell University, Ithaca, New York 14853

Received September 7, 2004; Revised Manuscript Received December 10, 2004

ABSTRACT: MntR is a metalloregulatory protein that helps to modulate the level of manganese in *Bacillus subtilis*. MntR shows a metal-response profile distinct from other members of the DtxR family of metalloregulatory proteins, which are generally considered to be iron(II)-activated. As part of an ongoing effort to elucidate the mechanism and metal-selectivity of MntR, several biophysical studies on wild-type MntR and two active site mutants, MntR E99C and MntR D8M, have been performed. Using circular dichroism (CD) spectroscopy, the thermal stability of these proteins has been examined in the presence of various divalent metal ions. Fluorescence intensity measurements of 8-anilino-1-naphthalenesulfonic acid (ANS) were monitored to examine the folding of these proteins in the presence of different metal ions. These experiments indicate that MntR undergoes a significant conformational change upon metal binding that results in stabilization of the protein structure. These studies also show that the MntR D8M active site mutation causes a detrimental effect on the metal-responsiveness of this protein. Fluorescence anisotropy experiments have been performed to quantify the extent of metal-activated DNA binding by these proteins to two different cognate recognition sequences. Binding of MntR and MntR E99C to the *mntA* cognate sequence closely parallels that of the *mntH* operator, confirming that the proteins bind both sequences with comparable affinity depending on the activating metal ion. Fluorescence anisotropy experiments on MntR D8M indicate significantly impaired DNA binding, providing additional evidence that MntR D8M is a dysfunctional regulator.

Metalloregulatory proteins, also known as metalloregulators, are a class of transcription factors that control gene expression in response to metal ions. The study of these proteins has increased dramatically in recent years, and metalloregulatory proteins have now been identified for many essential and toxic metal ions (*1*−*3*). Investigations of these metal-sensing proteins have improved our understanding of the central role they play in the metal ion homeostasis of microorganisms. We have focused our attention on MntR,[1] a manganese(II)-responsive transcription factor from *Bacillus subtilis* (*4*−*7*). MntR is one of a small number of manganese(II)-responsive members of the large DtxR family of metalloregulatory proteins, the majority of which are iron(II)-responsive systems (*8*−*10*). Other proteins in the DtxR family that have been assigned as potential manganese(II) sensors include ScaR, SirR, and TroR (*11*−*14*); all of these proteins are potentially useful candidates for elucidating how iron(II)- and manganese-(II)-activated DtxR proteins discriminate between these ions.

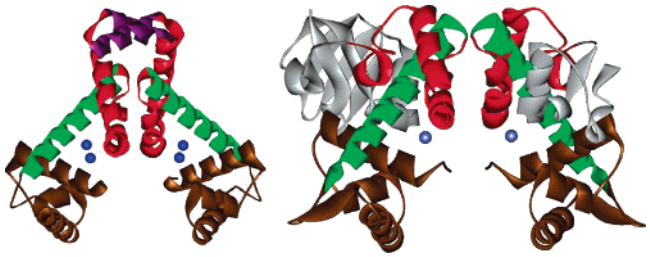

FIGURE 1: Ribbon representation of the crystal structures of holo MntR (left) and DtxR (right). Proteins are colored to highlight domains and function: helix−turn−helix DNA binding domain (brown), dimerization domain (red), linking α-helix (green), additional dimerization α-helix (purple, MntR only), and SH3-like domain (gray, DtxR only). Mn^{2+} and Co^{2+} ions are shown as spheres in the binding sites of MntR and DtxR, respectively. The Co^{2+} ion in the primary metal-binding site of DtxR is occluded by the protein backbone (lies between gray and green α-helices).

Earlier studies have demonstrated that MntR has a low affinity for the *mntH* regulatory sequence in the absence of transition metal ions (*4*, *5*). In the presence of divalent manganese or cadmium, MntR is strongly activated and demonstrates nanomolar affinity for the *mntH* consensus sequence (*6*). Oligomerization studies show no change in the quaternary structure of MntR in the apo or holo forms, revealing MntR to be a stable homodimer in solution (*6*). The crystal structure of MntR (Figure 1) shows that the monomer subunits interact through a substantial α-helical region (Asp123 to Lys136) at the C-terminal end of the polypeptides, which may explain the tight self-association of MntR (*15*). There are notable differences between the

† This work was supported by the University of California, San Diego, a Chris and Warren Hellman Faculty Scholar Award (S.M.C.), a Cottrell Scholar Award (S.M.C.), and NIH Grants GM-59323 (J.D.H.) and GM-60202-03 (T.C.D.).

* Author to whom correspondence should be addressed. Tel: (858) 822-5596. Fax: (858) 822-5598. E-mail: scohen@ucsd.edu.

‡ University of California, San Diego.

§ Cornell University.

[1] Abbreviations: ANS, 8-anilino-1-naphthalenesulfonic acid; CD, circular dichroism; DTNB, 5,5′-dithiobis(2-nitrobenzoic acid); DtxR, diphtheria toxin repressor; ICP-OES, inductively coupled plasma optical emission spectroscopy; MntR, manganese transport regulator from *B. subtilis*.

10.1021/bi0480741 CCC: $30.25
Published on Web 02/10/2005

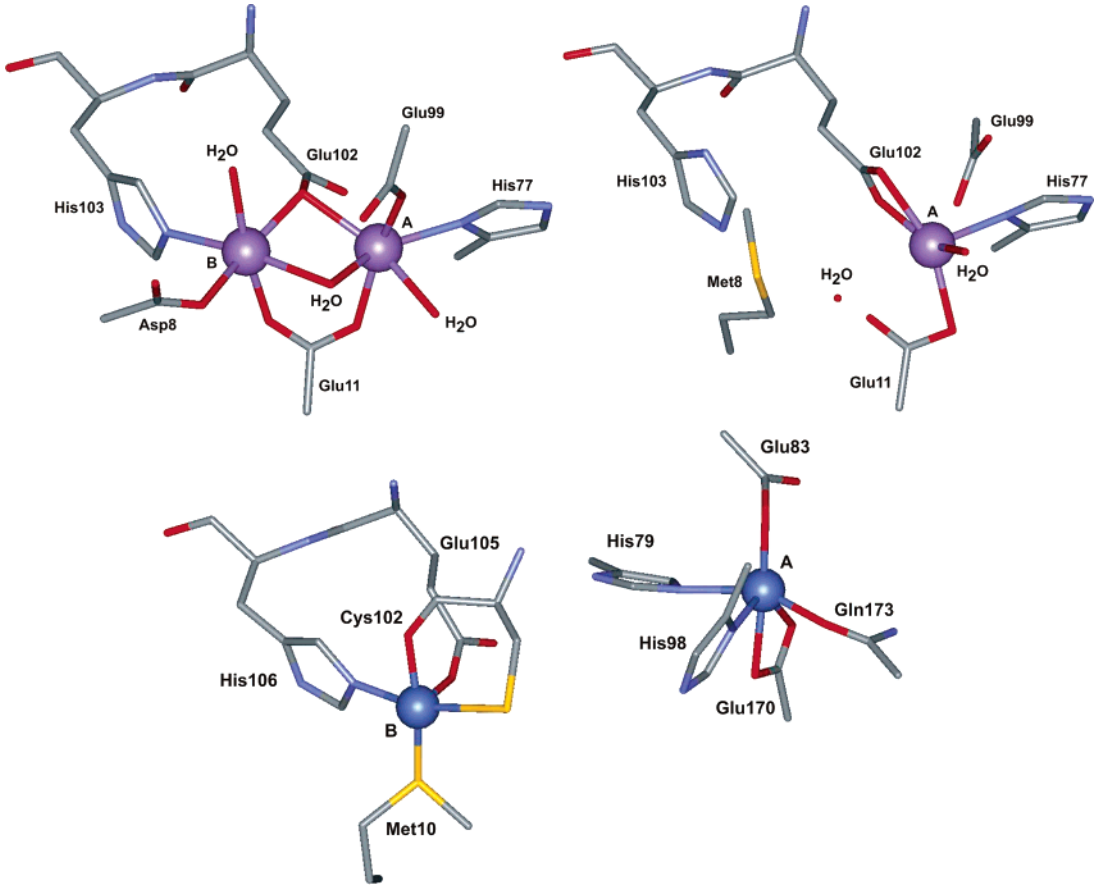

FIGURE 2: Metal-binding active sites for holo wild-type MntR (top left), MntR D8M (top right), and wild-type DtxR (bottom). The "primary" and "secondary" metal-binding sites are designated by A and B, respectively. Mn^{2+} and Co^{2+} ions are shown as spheres in the binding sites of MntR and DtxR, respectively. Adapted from refs *15* and *17*.

structure of MntR and other structurally characterized members of the DtxR family (Figure 1) of metalloregulatory transcription factors (*15*−*18*). DtxR, the prototypical iron-(II)-responsive member of this family found in *Corynebacterium diphtheriae*, is described as consisting of three domains: a DNA-binding, a dimerization, and an SH3-like domain. In contrast, MntR only has two major domains, a DNA-binding and a dimerization domain.

The most significant structural differences between DtxR and MntR are found in the metal-binding active site. DtxR and MntR are both found to bind two metal ions per protein monomer; however, the structure and positioning of these binding sites are notably different (Figure 2). The most obvious difference between the metal-binding sites is that DtxR has two distinct binding sites ($M^{2+}\cdots M^{2+}$ ∼9 Å) while MntR is found to have a single binuclear site ($Mn^{2+}\cdots Mn^{2+}$ 3.3 Å), with the metal ions bridged by two protein side chains and an aquo/hydroxo ligand (*15*). Sequence alignment of the two proteins shows that many of the ligating residues are conserved. The MntR active site recruits ligands generally conserved from the secondary site (site B in Figure 2) of DtxR, with only His77 from the primary site (site A in Figure 2). MntR was also found to use a new ligand Glu11, one of two glutamates that bridges the two manganese(II) ions (Figure 2). Interestingly, Glu11 is not conserved among iron-(II)-responsive members of the DtxR family nor among some suspected manganese(II)-responsive members of the family such as TroR (*11*, *15*). Three water molecules (one of which is bridging) are also found in the binuclear core of MntR.

The crystal structure of the mutant MntR D8M bound to Mn^{2+} has also been determined and demonstrates that the binuclear metal site is no longer present. Both Met8 and Glu99 are twisted away from their corresponding locations in the wild-type holoprotein, which results in an active site with only a single bound metal ion in a different coordination environment. The single Mn^{2+} ion in MntR D8M is coordinated by Glu11, His77, Glu102, and a water molecule in the A site of the protein (Figure 2). Despite the changes in the metal-binding site of MntR D8M, the overall protein fold is nearly identical to that of wild-type MntR (*15*).

Recent experiments have sought to address the issue of differential metal ion specificity in DtxR and MntR by mutagenesis and heterologous expression studies (*5*). These investigations demonstrated that both protein selectivity and the cellular environment contribute to the overall behavior in vivo. Interestingly, although mutation of key active site residues could convert DtxR from an iron(II)- to a manganese(II)-responsive repressor (DtxR M10D/C102E), mutagenesis of one (MntR D8M, MntR E99C) or both of the analogous MntR sites (MntR D8M/E99C) did not generate an iron(II)-selective response. In vivo, MntR E99C showed no ability to respond to Fe^{2+}, while MntR D8M was activated by Fe^{2+} to a slightly lesser degree than that obtained with Mn^{2+} (*5*). Why these MntR active site mutants failed to acquire Fe^{2+} sensitivity has not been resolved.

In an attempt to understand the effects of active site mutations on the metal-selective activation of MntR, this report details several in vitro experiments on wild-type MntR

and two of the previously reported active site mutants, MntR E99C and MntR D8M. Data presented in this study show that the active site changes in MntR E99C produce measurable, but not large differences in DNA-binding metal activation profiles, consistent with in vivo findings; however, several pieces of evidence are provided that show the behavior of MntR D8M to be notably different from that of the wild-type protein. These studies also shed light on the mechanism of MntR activation. Metal complexation is found to have a significant effect on MntR stability and structure, consistent with an allosteric mechanism whereby the MntR structure is reorganized and optimized for DNA recognition at the tertiary level upon metal binding.

EXPERIMENTAL PROCEDURES

General. All buffers were prepared using water purified through a Labconoco Water Pro Plus purification system. Buffers were degassed and sterilized by passing them through 0.22 μm filters. All biochemical reagents were obtained from commercial suppliers and were used as provided. $MnCl_2 \cdot 4H_2O$, $FeCl_2 \cdot 4H_2O$, $CoCl_2 \cdot H_2O$, $CdCl_2 \cdot H_2O$, and $NiCl_2 \cdot 6H_2O$ (99.99+%) were obtained from Aldrich. All protein chromatography was performed at 4 °C on an ÄKTA Prime biomolecule purification system (Amersham Pharmacia Biotech) using both inline UV and conductance detection. Matrix-assisted laser desorption time-of-flight (MALDI-TOF) mass spectrometry was performed by HT Labs (San Diego, CA) or at the core facility at the University of California, San Diego. The metal content/purity of all preparations of proteins, ultrapure water, buffers, and metal titrant solutions was determined as previously described (*6*) using a Perkin-Elmer Optima 3000 DV inductively coupled plasma optical emission spectrometer (ICP-OES) located at the Analytical Facility at the Scripps Institute of Oceanography. All fluorescence intensity and anisotropy experiments were performed on a Perkin-Elmer luminescence spectrometer LS 55 using a thermally jacketed cell holder that was maintained at 25 °C. Size-exclusion chromatography was performed on a calibrated HiLoad 16/60 Superdex 75 size-exclusion column (Amersham Pharmacia Biotech) as previously described (*6*). Analytical sedimentation equilibrium ultracentrifugation experiments were performed as previously described (*6*) on a Beckman XL-1 analytical ultracentrifuge located at the Biophysics Instrumentation Facility in the Department of Chemistry and Biochemistry at the University of California, San Diego. Oligonucleotides were purchased from Integrated DNA Technologies (Coralville, IA).

Expression and Purification of MntR. BL21-CodonPlus-(DE3)-RIL *E. coli* cells (Stratagene) transformed with pET17b plasmid containing the wild-type MntR (*4*) gene or the mutant genes MntR E99C or MntR D8M (*15*) were expressed and purified as previously described (*6*) with minor modifications. Buffers were as follows: lysis buffer consisted of 50 mM Tris, pH 8.0 at 4 °C, 200 mM NaCl, 5 mM EDTA, 5% (v/v) glycerol, 5 mM β-mercaptoethanol; cation exchange column buffer consisted of 50 mM HEPES, pH 7.0 at 4 °C, 150 mM NaCl, 5% (v/v) glycerol; storage buffer consisted of 20 mM HEPES, pH 7.2 at 4 °C, 200 mM NaCl, 5% (v/v) glycerol. MntR E99C and MntR D8M storage buffer also included 100 μM β-mercaptoethanol, and MntR D8M was stored at a higher salt concentration (300 mM NaCl) to prevent protein precipitation. The proteins were quantified using calculated extinction coefficients of 18910 M^{-1} cm^{-1} for wild type and MntR D8M, and 19035 M^{-1} cm^{-1} for MntR E99C (*19*).

Determination of Free Cysteines. MntR E99C was dialyzed for 2 × 4 h against deoxygenated storage buffer to remove β-mercaptoethanol contained in the original storage buffer for this mutant (vide supra). The dialysis was performed inside a glovebox containing a nitrogen atmosphere by using 500 μL capacity cassettes (Slide-A-Lyzer, 3.5 kDa MWCO, Pierce). A portion of the dialyzed protein sample (200 μL) was mixed with 200 μL of 7 M urea/2.5 M EDTA to give reaction mixtures containing 10−40 μM protein. To this mixture was added 25 μL of 2.5 mM 5,5′-dithiobis(2-nitrobenzoic acid) (DTNB) solution (prepared in storage buffer), and the mixture was agitated for 30 min. The reaction mixtures were taken out of the glovebox and analyzed spectrophotometrically by monitoring the absorbance at 412 nm using the reported extinction coefficient of 13600 M^{-1} cm^{-1} (*20*). The absorbance value at 412 nm was corrected by subtracting the spectrum of a buffer solution containing the same concentration of DTNB, but without any protein. MntR E99C preparations analyzed in this manner were found to contain 0.88 ± 0.12 free thiols per monomer.

Circular Dichroism Spectroscopy. Circular dichroism (CD) measurements were made on an AVIV circular dichroism model 202 spectrometer using a 2.0 mm quartz cuvette. The cuvettes were washed with soapy water, 1.0 M HCl, and copious amounts of ultrapure water followed by an ethanol rinse and air-drying to ensure that the cells were clean and free of metal contaminants. CD spectra (190−260 nm) were collected for each sample with a 0.5 nm step and a 4.0 s averaging time. Samples were supplemented with metal ions as desired from stock solutions (~5.0 mM) in storage buffer to a concentration of 1.0 mM. For thermal denaturation studies identical solution conditions were applied. The thermal denaturation profile for apo MntR was found to be identical in sodium phosphate or HEPES (storage) buffer (Figure S1, Supporting Information); however, under our experimental conditions the addition of metal ions to phosphate buffered solutions resulted in precipitation of metal phosphates. Therefore, the thermal denaturation experiments were performed in storage buffer to minimize complications with metal-binding experiments. Samples containing ~8 μM protein were heated from 50 to 100 °C at a rate of 1.0 °C/min, and ellipticity was monitored at 222 nm; melting temperatures (T_M) were determined as previously described (*21*). Select runs initiated at a lower starting temperature (25 °C) showed no difference in the denaturation curves. T_M values were calculated with eq 1 and solving for the temperature (T) at which $\Delta G = 0$:

$$\Delta G = -RT \ln[(I - I_F)/(I_U - I)] \quad (1)$$

where I is ellipticity at 222 nm at temperature T, I_F is the initial (folded) ellipticity, and I_U is the final (unfolded) ellipticity. Initial/folded intensity (I_F) and final/unfolded intensity (I_U) were taken from the first and last points of each individual denaturation curve. Due to lack of reversibility (nonequilibrium conditions) meaningful thermodynamic parameters could not be obtained. Data are presented as fractional change in ellipticity (FCE) at 222 nm by using eq 2:

$$\mathrm{FCE} = (I_F - I)/(I_F - I_U) \quad (2)$$

Fluorescence Emission with ANS. 8-Anilino-1-naphthalenesulfonic acid (ANS) (500 μM) and 5 μM protein sample in storage buffer (initial solution volume ~380 μL) were placed in a microcuvette (800 μL). Fluorescence spectra were collected using an excitation wavelength of 403 nm (slit width 15 nm) and an emission wavelength of 380−600 nm (slit width 20 nm). Data were an average of five scans. In the presence of protein, the emission maximum for ANS was found to blue shift 5−10 nm from the protein free value of 515 nm; therefore, comparative analysis of spectra was performed at 507 nm. Metal ions were added from stock solutions in storage buffer, to concentrations of approximately 0.1, 0.5, and 1.0 mM. Control experiments showed that under identical solution conditions, but in the absence of protein, no change in the fluorescence spectra of 500 μM ANS was observed in the presence of 1.0 mM Mg^{2+}, Ca^{2+}, Mn^{2+}, Co^{2+}, Ni^{2+}, or Cd^{2+}.

Fluorescence Anisotropy Titrations. The same procedure for preparing the double-stranded probe ds*mntH*26 was applied for both ds*mntH*26 and ds*mntA*26 used in this study (*6*). The modified oligonucleotide ss*mntA*26 (5′-6F-GATAATTTTGCATGAGGGAAACTTTC-3′, where the fluorescein dye is indicated by 6F = 6-carboxyfluorescein) and the complementary oligonucleotide (5′-GAAAGTTTCCCTCATGCAAAATTATC-3′) were used to generate the double-stranded oligonucleotide ds*mntA*26 containing the desired recognition sequence. The sequence of the labeled strand of ds*mntH*26 is 5′-6F-GAATAATTTGCCTTAAGGAAACTCTC-3′. Fluorescence anisotropy experiments were performed as previously described with some modifications (*6*). Measurements were collected with an excitation wavelength of 492 nm (slit width 15 nm), an emission wavelength of 520 nm (slit width 20 nm), and a 1.0 s integration time. The *g*-factor for all of the experiments was 1.15 ± 0.08. For titrations in the presence of 1.0 mM Fe^{2+} the experiments were performed by using an anaerobic cell assembled inside a glovebox with a nitrogen atmosphere. The r_{obs} versus $[MntR]_{total}$ data were fit to a 1:1 binding isotherm model (nondissociable dimer) (*6*) by using least-squares regression analysis software (Synergy KaleidaGraph).

RESULTS

Preparation and Characterization of MntR E99C and MntR D8M. The MntR E99C and MntR D8M mutants were characterized by MALDI-TOF-MS, analytical sedimentation equilibrium ultracentrifugation, size-exclusion (SE) chromatography, and circular dichroism (CD) spectroscopy. Analytical sedimentation ultracentrifugation absorbance data were fit to a single, idealized species (Figure S2, Supporting Information). Apparent molecular weights for MntR E99C and MntR D8M were 35284 ± 1351 and 33529 ± 1723, in good agreement with the expected values for protein homodimers of 33438 and 33522, respectively. In addition, evaluation by size-exclusion chromatography was consistent with the proteins eluting as homodimers with apparent molecular weights in the range of 33−35 kDa (data not shown). The proteins were characterized by MALDI-TOF mass spectrometry; MntR E99C generated two peaks at *m*/*z* 16745 Da $[M + Na]^+$ (calculated 16742 Da) and 16610 Da $[M - Met + Na]^+$, the latter peak characteristic of the protein with the N-terminal methionine residue truncated (calculated 16611). MntR D8M generated a single peak at *m*/*z* 16648 Da $[M - Met + Na]^+$ (calculated 16653), indicating that the peak corresponds to MntR D8M with the N-terminal methionine residue truncated. Analysis of MntR E99C with Ellman's reagent (DTNB) gave a value of 0.88 ± 0.12 free thiol per monomer (1 free thiol expected), consistent with at least ~90% of the protein being in the properly reduced form. CD spectroscopy of MntR, MntR E99C, and MntR D8M in sodium phosphate buffer showed the expected features at 208 and 222 nm (Figure S3, Supporting Information) characteristic of a highly α-helical secondary structure (*6*, *15*). As found with wild-type MntR (*6*), addition of Mn^{2+} to MntR E99C or MntR D8M (data not shown) did not produce significant changes in the 222 nm feature in the CD spectrum (*22*).

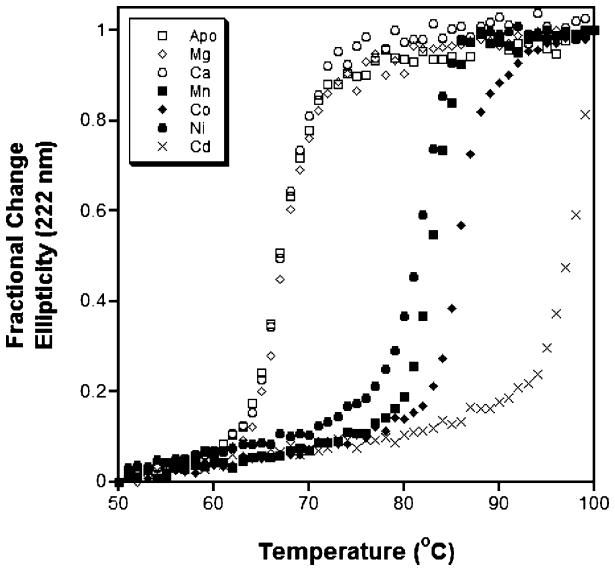

FIGURE 3: Thermal denaturation curves for wild-type MntR (8 μM) monitored by CD spectroscopy at 222 nm: unfolding of apo MntR (open squares) and of MntR in the presence of 1.0 mM Mg^{2+} (◇), Ca^{2+} (○), Mn^{2+} (■), Co^{2+} (◆), Ni^{2+} (●), and Cd^{2+} (×). Buffer = 20 mM HEPES, pH 7.2 at 4 °C, 200 mM NaCl, 5% (v/v) glycerol. Path length = 2 mm.

Thermal Denaturation Studies Using Circular Dichroism Spectroscopy. Binding of Mn^{2+} does not significantly alter the secondary structure composition of these proteins. As a means to determine what, if any, effect metal binding had on the structure of MntR, thermal denaturation experiments were performed on these proteins in the apo and holo forms. Stabilization of protein structure upon metal binding has been found to be important for the metalloregulatory protein NikR (*23*). The thermal melting of the proteins was followed by CD spectroscopy at the maximal ellipticity of 222 nm. Heating of MntR at a rate of 1 °C per minute resulted in a clear melting transition and loss of the CD signal (Figure 3). Visible inspection of the sample upon complete denaturation revealed precipitation of MntR, and consistent with this observation, the protein could not be refolded upon cooling (CD signal did not return upon cooling, data not shown). The folding is not reversible; therefore, the system is not under equilibrium conditions (*21*); however, the midpoint of the denaturation curve was reproducible and a melting temperature (T_M) of ~67 °C was obtained for apo MntR (Table 1). Addition of 1.0 mM Mn^{2+} to the solution

Table 1: Melting Transition Temperatures (T_M) for MntR Proteins Obtained from Circular Dichroism Measurements during Thermal Denaturation in the Presence of Various Divalent Metal Ions[a]

metal ion (1 mM)	MntR (°C)	MntR E99C (°C)	MntR D8M (°C)
Apo (no metal)	67	73	68
Mg^{2+}	67	72	67
Ca^{2+}	68	72	67
Mn^{2+}	83	77	76
Co^{2+}	86	89	85
Ni^{2+}	81	87	76
Cd^{2+}	>90[b]	>100[b]	84

[a] All values are based on an average of at least two independent experiments. All values are reproducible to ±1 °C. [b] Complete denaturation was not observed up to 100 °C, and a satisfactory endpoint could not be obtained.

resulted in a significant thermal stabilization of MntR, with a T_M of ~83 °C. Similar increases were found in the presence of Co^{2+} and Ni^{2+}, but not upon addition of Mg^{2+} or Ca^{2+}, demonstrating that the observed stabilization is specific to activation by transition metal ions (*6*). Addition of 1.0 mM Cd^{2+} resulted in enhanced stabilization of the protein with only partial melting observed above 90 °C.

Thermal denaturation experiments with MntR E99C were generally comparable to that found with wild-type protein (Table 1), with two notable exceptions. First, in the presence of 1.0 mM Mn^{2+}, the melting transition of MntR E99C showed biphasic behavior (Figure S4, Supporting Information); the origin of this biphasic behavior is presently unknown. Second, addition of 1.0 mM Cd^{2+} stabilizes MntR E99C such that no melting transition is observed up to 100 °C. In contrast, MntR D8M showed significant changes in thermal stabilization behavior relative to wild-type MntR (Table 1). MntR D8M was far less stabilized by the presence of 1.0 mM Mn^{2+}, with only a ~8 °C increase in T_M compared to a ~16 °C increase with wild-type MntR. The stabilization obtained with Ni^{2+} is also reduced relative to wild type; moreover, unlike wild-type MntR or MntR E99C, MntR D8M undergoes a melting transition at ~84 °C in the presence of 1.0 mM Cd^{2+} (Figure S4). These thermal denaturation studies were the first indicators that MntR D8M has notably different behavior from the other proteins investigated here.

Conformation Changes Monitored by ANS Fluorescence. The data obtained from thermal denaturation CD experiments indicated that activating metal ions were able to stabilize the structure of wild-type MntR. To gain further insight into the nature of this stabilization, fluorescence studies with 8-anilino-1-naphthalenesulfonic acid (ANS) were performed. ANS is a fluorescent chromophore known to bind to hydrophobic surfaces of proteins. Binding of ANS to hydrophobic surfaces increases its fluorescence intensity, while exclusion from such surfaces (i.e. upon protein folding or structural rearrangement) results in a decrease in fluorescence emission (*21*, *24*). Therefore, ANS can be used to monitor changes in the tertiary structure (hydrophobic packing) of proteins. ANS has been successfully used to examine the solution structure of DtxR (*25*). The combination of 5 μM apo MntR and 500 μM ANS solution results in a ~54% increase in fluorescence intensity versus ANS alone (Figure 4). Subsequent addition of 0.1, 0.5, and 1.0 mM Mn^{2+} results in a reduction of fluorescence intensity to 34%, 15%, and 12%, respectively, above that of ANS alone. The

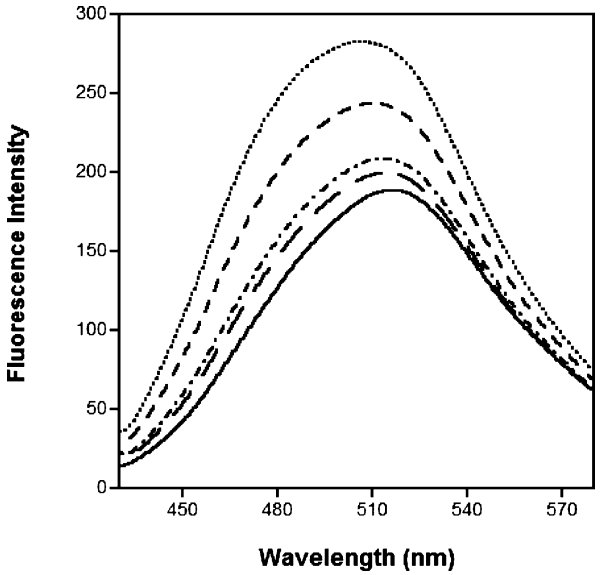

FIGURE 4: ANS fluorescence spectra in the presence of wild-type MntR and variable amounts of Mn^{2+}. The solid line is the initial spectrum of ANS (500 μM) without addition of protein or metal ion. Other spectra are upon addition of 5 μM MntR (dotted line), 5 μM MntR and 0.1 mM Mn^{2+} (narrow dashed line), 5 μM MntR and 0.5 mM Mn^{2+} (dotted−dashed line), and 5 μM MntR and 1.0 mM Mn^{2+} (wide dashed line). λ_{ex} = 403 nm. Buffer = 20 mM HEPES, pH 7.2 at 4 °C, 200 mM NaCl, 5% (v/v) glycerol. T = 25 °C.

loss in fluorescence intensity is not due to quenching from the metal ion, as exposure of ANS to 1.0 mM Mn^{2+} in the absence of MntR has no effect on fluorescence emission (data not shown). Therefore, the observed fluorescence decreases are indicative of changes in protein structure. Figure 5 summarizes the data for MntR, MntR E99C, and MntR D8M in the presence of ANS and Mn^{2+}, Cd^{2+}, Co^{2+}, and Ni^{2+} at concentrations of 0, 0.1, 0.5, and 1.0 mM. Mg^{2+} and Ca^{2+} showed no significant affect on ANS fluorescence (data not shown), consistent with the inability of these metal ions to activate or stabilize MntR. By comparison, MntR appears to undergo a complete structural rearrangement in the presence of 0.1 mM Co^{2+} or Cd^{2+}, as indicated by a large drop in fluorescence intensity; there were no further substantive changes upon addition of higher concentrations of these metal ions. MntR requires slightly higher concentrations of Mn^{2+} (~0.5 mM) to achieve saturation. Ni^{2+} fails to significantly reduce ANS fluorescence even at concentrations of 1.0 mM. In contrast, MntR E99C shows complete fluorescence reduction, upon addition of 0.1 mM Ni^{2+}, Co^{2+}, or Cd^{2+}, but requires the presence of 1.0 mM Mn^{2+} to achieve the same effect. The increased ability of Ni^{2+} to activate MntR E99C relative to wild-type MntR is in agreement with data obtained from fluorescence anisotropy DNA binding studies (vide supra).

Consistent with thermal denaturation experiments presented above, the ANS fluorescence experiments suggest that MntR D8M is structurally and functionally deficient. Although MntR D8M appears to fold in the presence of Co^{2+}, the response to Mn^{2+} is significantly reduced. Furthermore, addition of 0.1 mM Cd^{2+} results in an initial reduction in fluorescence intensity, followed by protein precipitation at higher concentrations (manifested as an increase in fluorescence intensity due to scattered light, Figure 5). Like wild-type MntR, MntR D8M shows little change in ANS

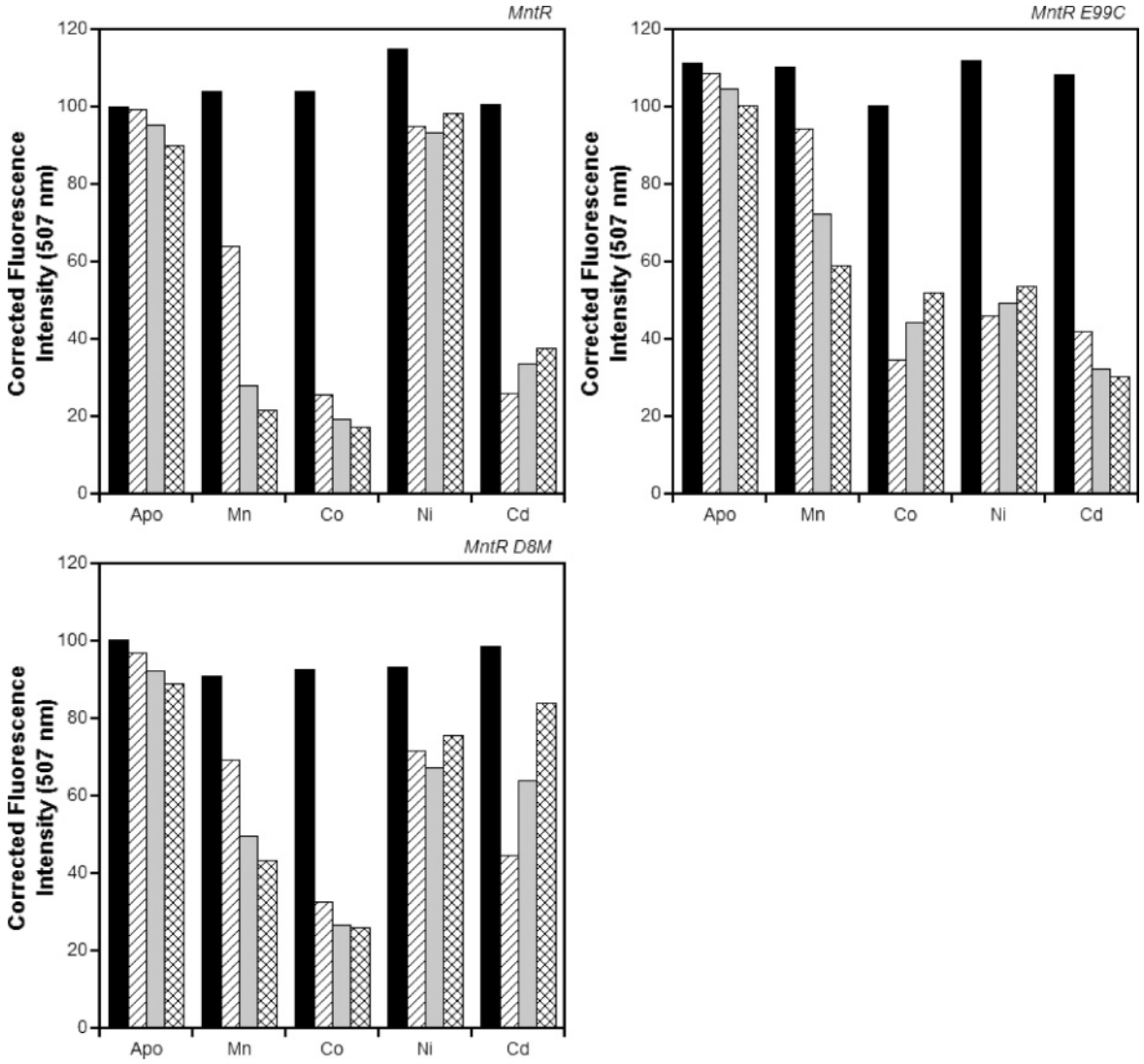

FIGURE 5: Changes in ANS fluorescence intensity (507 nm) in the presence of MntR proteins. Plots are labeled for MntR, MntR E99C, and MntR D8M. Bars represent addition of 0 (black), 0.1 (single slash), 0.5 (gray), and 1.0 (crossed slash) mM of the metal ion listed. The column labeled Apo contained ANS and protein only diluted with an equivalent volume of metal-free buffer. All intensities have been background corrected by subtracting the fluorescence intensity of a solution containing an identical concentration of ANS in buffer alone. All samples are the results of at least two independent experiments. $\lambda_{ex} = 403$ nm. Buffer = 20 mM HEPES, pH 7.2 at 4 °C, 200 mM NaCl, 5% (v/v) glycerol. $T = 25$ °C.

fluorescence in the presence of excess Ni^{2+}. The ANS data indicate either that MntR D8M does not undergo a substantial structural change upon binding certain metal ions or that it is perhaps deficient in its abilities to bind these ions.

DNA Binding of MntR. Fluorescence anisotropy studies of MntR and the *mntH* recognition sequence have been previously used to quantify DNA binding affinity in the presence of various metal ions (*6*, *26*). In an effort to expand upon these earlier results, the binding of MntR to ds*mntH*26 was studied in the presence of Co^{2+} and Fe^{2+}, which were not examined in our earlier report. K_d values were obtained by fitting the fluorescence anisotropy data to a simple 1:1 binding isotherm (*6*), and were in good agreement with the experimental data. The data indicate that both Co^{2+} and Fe^{2+} are intermediate level activators of MntR, better than Ni^{2+}, Cu^{2+}, and Zn^{2+}, but less effective than Mn^{2+} and Cd^{2+} (Table 2). In contrast to in vivo studies (*5*), these experiments show that MntR can be activated by Fe^{2+}; however, the present experiments are performed in the presence of a large excess of metal ion. Binding to ds*mntH*26 was sequence specific, as a 500-fold excess calf thymus DNA did not interfere with binding of manganese(II)-activated MntR (data not shown). Binding of MntR to the *mntA* sequence was investigated by using a labeled, 26-base pair oligonucleotide (ds*mntA*26) containing the core recognition sequence 5′-6F-GATAATT-TTGCATGAGGGAAACTTTC-3′. The *mntA* sequence is the operator sequence in *B. subtilis* that controls expression of the ABC transporter *mntABCD* (*4*). As shown in Table 3,

Table 2: Binding of MntR, MntR E99C, and MntR D8M Proteins to the *mntH* Recognition Sequence[a]

metal ion (1 mM)	MntR K_d (nM)[b]	MntR E99C K_d (nM)[b]	K_{d-wt}/K_{d-E99C}	MntR D8M K_d (nM)[b]	K_{d-wt}/K_{d-D8M}
Apo	>8000[c,d]	>3200[c]	n/a	>4900[c]	n/a
Mn^{2+}	16.0 ± 0.4[d]	36.0 ± 4.9	0.4	204 ± 37.3	0.1
Fe^{2+}	87.2 ± 4.2	139 ± 28	0.6	458 ± 2	0.2
Co^{2+}	193 ± 30	52.3 ± 11.9	3.7	490 ± 81	0.4
Ni^{2+}	2342 ± 305[d]	298 ± 70	7.9	∼3000[c]	n/a
Cd^{2+}	7.3 ± 1.1[d]	24.1 ± 3.6	0.3	64.1 ± 8.1	0.1

[a] Dissociation constants (K_d) for modeling the fluorescence anisotropy data with a 1:1 binding isotherm. All values are based on an average of at least two independent experiments. [b] Standard deviations also listed. [c] Estimated, saturation not observed. [d] From ref *6*.

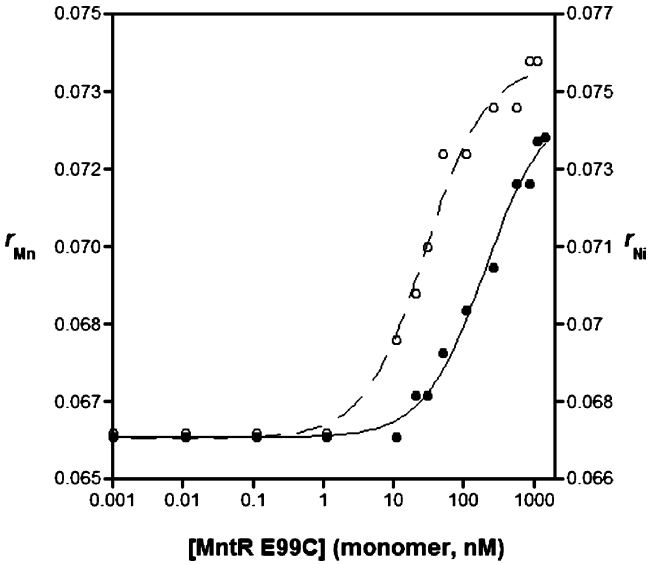

FIGURE 6: Representative fluorescence anisotropy data for MntR E99C binding to the oligonucleotide ds*mntH*26: binding in the presence of 1.0 mM Mn^{2+} (○) and Ni^{2+} (●). Lines through each set of points represent a fit of the data to a 1:1 oligonucleotide/dimer binding isotherm. [ds*mntH*26] = 10 nM. Buffer = 20 mM HEPES pH 7.2 at 4 °C, 500 mM NaCl, 5% (v/v) glycerol. T = 25 °C.

Table 3: Binding of MntR, MntR E99C, and MntR D8M Proteins to the *mntA* Recognition Sequence[a]

metal ion (1 mM)	MntR K_d (nM)[b]	MntR E99C K_d (nM)[b]	K_{d-wt}/K_{d-E99C}	MntR D8M K_d (nM)[b]	K_{d-wt}/K_{d-D8M}
Apo	>3500[c]	>3500[c]	n/a	>3500[c]	n/a
Mn^{2+}	30.4 ± 1.3	25.8 ± 6.4	1.2	93.0 ± 23.8	0.3
Fe^{2+}	79.8 ± 20.8	103 ± 12	0.8	267 ± 26	0.3
Co^{2+}	81.5 ± 13.8	26.4 ± 5.1	3.1	241 ± 27	0.3
Ni^{2+}	507 ± 38	94.8 ± 9.4	5.4	1122 ± 151	0.4
Cd^{2+}	24.3 ± 4.6	19.8 ± 6.0	1.2	37.7 ± 4.8	0.6

[a] Dissociation constants (K_d) for modeling the fluorescence anisotropy data with a 1:1 binding isotherm. All values are based on an average of at least two independent experiments. [b] Standard deviations also listed. [c] Estimated, saturation not observed.

MntR binds ds*mntA*26 in the presence of either 1.0 mM Mn^{2+} or Cd^{2+} with only slightly weaker affinity than found for ds*mntH*26. The intermediate (Co^{2+} and Fe^{2+}) and weak activators (Ni^{2+}) stimulate MntR to bind the *mntA* sequence with slightly improved affinity than found with *mntH*, but the overall trend is essentially unchanged with $Cd^{2+} \approx Mn^{2+} > Fe^{2+} \approx Co^{2+} \gg Ni^{2+} \gg$ apo.

The binding of MntR E99C was also studied using the ds*mntH*26 and ds*mntA*26 oligonucleotides (Figure 6). Surprisingly, the affinity of MntR E99C for both oligonucleotides was essentially unchanged from that found for wild-type MntR in the presence of Mn^{2+}, Fe^{2+}, and Cd^{2+} (Tables 2 and 3). This data is consistent with the earlier finding that both MntR and MntR E99C did not respond to Fe^{2+} in vivo (*5*). The DNA binding ability in the presence of Co^{2+} and Ni^{2+} improved between 3- to 8-fold over wild type for both sequences. As expected, control titrations with MntR E99C in the presence of 1.0 mM Ca^{2+} and Mg^{2+} showed no significant DNA binding to either sequence (data not shown).

Lastly, fluorescence anisotropy studies of MntR D8M clearly showed the deficient function of this active site mutant. Activation of MntR D8M by all transition metal ions showed reduced affinities for both cognate sequences (Tables 2 and 3), with a greater impact on the affinity toward ds*mntH*26. For example, the affinity of MntR D8M for ds*mntH*26 in the presence of 1.0 mM Mn^{2+} was reduced by more than 10-fold relative to wild type (Figure S5, Supporting Information). Although the overall metal selectivity appeared similar to wild-type MntR (vide supra), MntR D8M was clearly deficient in DNA binding relative to the other proteins examined. The fluorescence anisotropy data for MntR D8M provide additional evidence that this mutation causes a substantial change in the protein that manifests as both structural and functional anomalies.

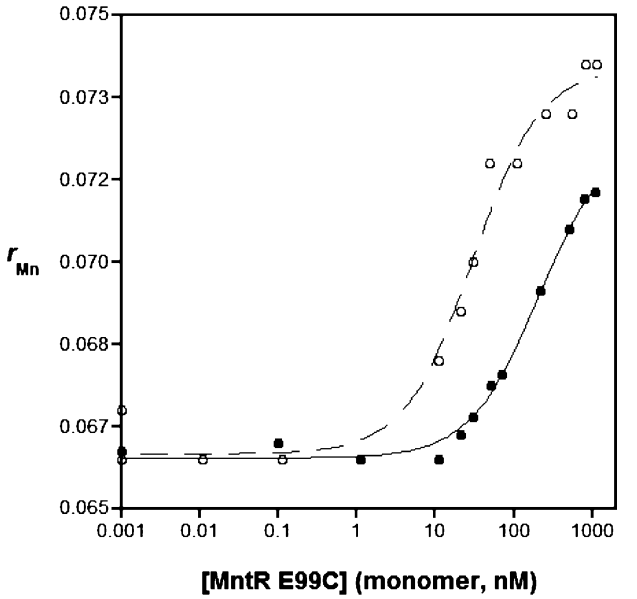

FIGURE 7: Representative fluorescence anisotropy data for MntR E99C binding to the oligonucleotide ds*mntH*26: binding in the presence of 1.0 mM Mn^{2+} (○) and 0.1 mM Mn^{2+} (●). Lines through each set of points represent a fit of the data to a 1:1 oligonucleotide/dimer binding isotherm. Data show that binding affinity for ds*mntH*26 drops when the concentration of Mn^{2+} is reduced. [ds*mntH*26] = 10 nM. Buffer = 20 mM HEPES pH 7.2 at 4 °C, 500 mM NaCl, 5% (v/v) glycerol. T = 25 °C.

Experiments with ANS fluorescence showed that the MntR proteins underwent differing degrees of structural organization based on the concentration and nature of added metal ion. For example, at 0.1 mM Cd^{2+} MntR E99C appears completely folded, while the same concentration of Mn^{2+} appears insufficient to induce significant folding (Figure 5). Nevertheless, at high concentrations of either metal (1.0 mM), MntR E99C showed strong activation for DNA-binding with nearly equal affinity for the cognate sequences *mntH* and *mntA*. These observations suggested that the differences observed in the ANS experiments are likely due to differences in metal-binding affinity. To further examine this hypothesis, DNA-binding fluorescence anisotropy experiments with MntR E99C and ds*mntH*26 were performed at reduced metal concentrations. Binding of ds*mntH*26 by MntR E99C with 0.1 or 0.01 mM Cd^{2+} ($K_d \approx$ 19 and 26 nM, respectively) was essentially identical to that found in the presence of 1.0 mM Cd^{2+} (Figure S6, Supporting Information). In contrast, the DNA-binding ability of MntR E99C with 0.1 mM Mn^{2+} was significantly reduced with a K_d value of ~209 nM (Figure 7). This suggests that MntR E99C binds $Cd^{2+}$with higher affinity than Mn^{2+}, even though at high concentrations both metals are comparable activators for DNA binding.

DISCUSSION

Mechanism of MntR Activation. Addition of activating metal ions to MntR does not measurably change the CD feature at 222 nm, suggesting that the largely α-helical secondary structure of MntR does not require, nor is substantially altered by, metal binding. In contrast, the thermal stability of the protein, as evaluated by CD spectroscopy, is significantly enhanced by the presence of activating metal ions such as Mn^{2+} and Cd^{2+}. Metal ions such as Mg^{2+} and Ca^{2+}, which do not activate the protein for DNA binding, have no effect on protein stability. These CD experiments indicate that although the secondary structure of MntR is not metal ion dependent, metal binding greatly stabilizes these structural features. Similar observations have been made with the nickel(II)-responsive metalloregulator NikR, where certain transition metal ions are found to stabilize one domain of NikR, with Ni^{2+} showing a selective ability to stabilize both domains of the protein (*23*).

ANS fluorescence experiments with MntR clearly demonstrate that metal binding results in a considerable reduction of the available hydrophobic surface area and generation of a more compact protein fold. This observation is consistent with ANS experiments performed on an iron(II)-responsive homologue DtxR (*25*). The ANS fluorescence data indicate that apo MntR undergoes a significant structural rearrangement upon metal coordination that leads to allosteric activation of the protein for DNA binding; however, while ANS binding allows us to stipulate that the fluorescence quenching occurs due to a decrease of available hydrophobic surface that accompanies protein reorganization, the pathway and origin of this rearrangement cannot be unambiguously determined. One possibility is that this organization stems from a rearrangement of the quaternary structure of MntR. Although apo MntR is a stable homodimer (*6*), the observed reorganization may occur by a reorientation of the two monomer subunits relative to one another, optimizing the orientation and spacing of the helix−turn−helix motifs for DNA binding and reducing the amount of exposed hydrophobic surface in the process. This type of quaternary structural compaction has been observed in SmtB, a zinc-responsive metalloregulatory protein of the ArsR family (*3*, *27*). SmtB is a negatively regulated repressor of transcription from cyanobacteria that has a high affinity for its cognate DNA sequence in the apo form and a reduced affinity upon metal binding. Crystallographic and NMR solution studies show that zinc(II) binding to SmtB causes a quaternary structural contraction that places the DNA recognition elements in a suboptimal conformation (*27*). A second possibility is that MntR undergoes an internal tertiary structural rearrangement that results in a loss of exposed hydrophobic surface area that leads to an optimized MntR structure for DNA binding. Such a tertiary structural rearrangement for MntR may originate from a molten globule-like state with defined secondary structural elements, but a less organized tertiary structure (*28*). This scenario has been proposed for DtxR, where the protein was observed to be in a molten globule state prior to metal binding (*25*).

When viewed in the context of the available structural data on MntR (*15*) and the observation that apo MntR exists as a stable homodimer (*6*), we favor a model that invokes a change in tertiary conformation of MntR that acts as an allosteric trigger for DNA binding. Such a model is consistent with the observation that the metal-binding site in MntR recruits ligands from every major structural region of the protein: Asp8 and Glu11 from the helix−turn−helix DNA binding domain (Figure 1, brown), Glu99, Glu102, and His103 from the dimerization domain (Figure 1, red), and His77 from the long α-helix that links the dimerization and DNA binding domains (Figure 1, green). It is feasible that binding of a metal ion to this active site leads to a widespread structural rearrangement of the protein secondary structures to form a stable, activated repressor complex. This is also consistent with the generally defective behavior of MntR D8M, which alters and lacks several of these key binding interactions (Figure 2), rendering it incapable of completely organizing the protein tertiary structure upon binding of a transition metal ion (vide infra). Whether this tertiary structure reorganization originates from a molten globule state or from a relatively well-structured MntR conformation will best be resolved by NMR solution studies.

CD thermal denaturation and ANS fluorescence experiments suggest that the mechanism of repressor activation is related to substantial ordering and stabilization of the protein structure at the tertiary level. The significance of these findings is illustrated by comparison to other metalloregulatory proteins such as DtxR and CzrA. X-ray diffraction studies of both the apo and holo forms of DtxR show minimal variance in structure (*29*), making it difficult to account for functional differences between the two forms or gain insight into the metal-mediated activation of the protein. X-ray structural characterization of the metalloregulatory protein CzrA also shows nominal changes in overall structure between the apo and holo forms (*27*), again limiting functional and mechanistic insight. An improved understanding of metal activation for both DtxR and CzrA was ultimately obtained through solution studies. In the case of DtxR, metal binding was found to organize the tertiary structure into a favorable configuration in a disorder-to-order transition (*25*). For CzrA metal complexation resulted in reduced structural dynamics that served to "freeze out" a configuration required for DNA binding (*27*). The studies on DtxR and CzrA highlight the importance of our experiments with MntR, as the significant structural changes found for MntR in solution have not been previously investigated and appear to be an important part of the metal-mediated mechanism for DNA binding. Further investigation into solution dynamics of MntR using NMR spectroscopy will provide a more complete understanding into the mechanism of activation.

DNA Binding Selectivity. Apo MntR has a low affinity for both the *mntH* and *mntA* cognate sequences, as judged by fluorescence anisotropy measurements. Binding of MntR is dependent on the presence of transition metal ions with the general trend for DNA-binding ability (at 1.0 mM metal ion) following $Cd^{2+} \approx Mn^{2+} > Fe^{2+} \approx Co^{2+} \gg Ni^{2+} \gg$ apo. These findings are consistent with an earlier hypothesis that MntR acts as a manganese(II)-regulated repressor of both the *mntH* and *mntABCD* operons, confirming previous studies using DNase I footprinting experiments (*7*). The binding studies presented here also show that MntR generally has comparable affinities for the *mntH* and *mntA* sequences when activated by transition metal ions. The two new metal ions investigated in this study, Fe^{2+} and Co^{2+}, were found to be intermediate activators, indicating that there is a gradation

of levels to which MntR can be activated to bind DNA. Overall, the metal-selective response of MntR appears somewhat more stringent with *mntH*, as activation with excess Mn^{2+} is ~150-fold more effective than Ni^{2+}, while excess Mn^{2+} activates MntR only ~17-fold more strongly than Ni^{2+} for *mntA*. The presence of excess metal ion in the fluorescence anisotropy experiments limits unambiguous interpretation of the data and makes the origin of metal-selective activation unclear; however, evidence suggests (vide infra) that differences in metal-binding affinities alone (*5*) are insufficient to explain the metal specific response of MntR (M. V. Golynskiy and S. M. Cohen, unpublished results).

As found in earlier reports, MntR is best activated by two very disparate metal ions, Mn^{2+} and Cd^{2+} (*4*, *6*). Why MntR responds so strongly to these metal ions and why the Cd^{2+} response may be biologically relevant is a topic of particular interest. Interestingly, DNA-binding experiments performed at reduced metal concentrations provide some likely insight into the metal-binding affinities of MntR, which may serve to address the latter question. In the presence of 1.0 mM Mn^{2+} or Cd^{2+}, MntR E99C binds ds*mntH*26 with comparable affinity. In contrast, at 0.1 mM Mn^{2+} affinity drops ~10-fold, but remains essentially unchanged with Cd^{2+} even at concentrations as low as 0.01 mM metal. Although experiments with wild-type MntR need to be performed to further validate this observation, this finding supports the hypothesis that metal ion affinity does play a role in the metal-selective response of MntR (*5*). A greater affinity for Cd^{2+} may play an important physiological role for MntR. The proton-dependent Mn^{2+} transporter MntH has been shown to facilitate Cd^{2+} uptake in *B. subtilis* (*4*). If Cd^{2+} is assumed to be a nonessential, and likely toxic, metal ion for this organism, then it would be important that MntR be able to respond to small amounts of Cd^{2+} inadvertently taken up through the MntH transporter in a cadmium(II)-contaminated environment. Furthermore, the sensitivity of MntR to Cd^{2+} may also explain why *B. subtilis* has several pathways for Mn^{2+} uptake (*4*). In the presence of small amounts of Cd^{2+}, the MntH (and MntABCD) transport system would be repressed to prevent transport of the toxic metal, but alternative pathways might still allow for essential quantities of Mn^{2+} to be taken into the cell.

Active Site Mutants. Recent in vivo studies have been helpful in clarifying the role and origin of the metal-selective response by MntR and DtxR. Although the normally iron(II)-responsive DtxR could be changed to a manganese(II)-selective mutant, mutants of MntR were always found to be manganese(II)-responsive (*5*). In reporter gene assays, Mn^{2+} remained the preferred activator for both MntR E99C and MntR D8M; however, MntR E99C showed no gene repression in response to Fe^{2+}, while MntR D8M could be activated by Fe^{2+}, albeit at higher concentrations than required with Mn^{2+} (*5*). The fluorescence anisotropy binding experiments to ds*mntH*26 described here with MntR E99C and MntR D8M are qualitatively consistent with the in vivo findings. Relative binding affinities for both cognate sequences in the presence of Mn^{2+} and Fe^{2+} remain essentially unchanged between MntR and MntR E99C. In contrast, MntR D8M shows a marked loss of selectivity for Mn^{2+}, suggesting that a loss of Mn^{2+} sensitivity and not a gain of Fe^{2+} function is responsible for the in vivo responsiveness of this mutant to both Mn^{2+} and Fe^{2+} in *B. subtilis*.

The biophysical studies on MntR D8M presented here show that this mutation is highly detrimental to the function of this transcription factor. Thermal denaturation studies demonstrate that apo MntR D8M has a similar denaturation transition temperature to wild type; however, MntR D8M is far less resistant to thermal denaturation in the presence of Mn^{2+}, Ni^{2+}, and Cd^{2+}. Experiments with the fluorescent probe ANS support the thermal denaturation results, as Mn^{2+}, Ni^{2+}, and Cd^{2+} induce a smaller decrease in ANS fluorescence in MntR D8M when compared to wild-type MntR. ANS data indicate that only Co^{2+} retains a good ability to organize MntR D8M (Figure 5), and this is consistent with the thermal denaturation curves that show Co^{2+} stabilization of MntR D8M to be the least perturbed when compared to wild type (Table 1). Giedroc and co-workers have discussed active site mutations of metalloregulators in the context of SmtB/ArsR family of proteins, and they have provided three possible explanations for the defective activity of mutant proteins (*3*): (a) the mutant has lost the ability to bind metal ions; (b) the mutant protein binds metal ions, but with substantially reduced thermodynamic affinity; or (c) the mutant binds metal ions with high affinity, but in a non-native coordination geometry that results in a nonfunctional protein. The binuclear nature of the native MntR binding site somewhat complicates this classification scheme, but clearly MntR D8M has not completely lost the ability to bind metal ions as shown by the experiments described herein, as well as the crystal structure of holo MntR D8M, where one of the two metal-binding sites was found to be occupied (*15*). Under the experimental conditions employed here, which utilize a large excess of metal ion, it is not possible to unambiguously determine which of the remaining possibilities is most relevant to MntR D8M. The crystal structure of MntR D8M shows a single manganese(II) ion bound in a somewhat modified coordination environment (Figure 2), but whether this site retains a high affinity for metal binding has not yet been determined.

Overall, our findings are consistent with the structure of holo MntR D8M (Figure 2), which shows a disruption of the binuclear metal-binding site (*15*). DNA binding studies with MntR D8M show that this protein is functionally deficient, showing only weak activation upon binding of transition metal ions. The results obtained here and the reported X-ray structure of MntR D8M suggest that occupation of metal-binding site B may be essential for proper function of the protein (*15*). The deficiencies in MntR D8M behavior observed here do lend support to the hypothesis that the binuclear site is an important factor in activating MntR, at least in the case of Mn^{2+}. While at present it is unclear exactly which aspects of the metal site in MntR are required for gene repression, the binuclear nature of the active site makes it unique among the DtxR family of metalloregulatory proteins that have been structurally characterized to date (*15*−*18*, *30*). Indeed, several metalloregulatory proteins that function as positively regulated repressors of transcription are known to employ more than one metal ion per monomer, but do so in two distinct metals sites. These sites can be broadly categorized into two groups, a high affinity "structural" site and a lower affinity "sensory" or "allosteric" site. For example, in NikR a high affinity site activates the protein to bind DNA when occupied by a variety of metal ions; however, a second low affinity site in NikR is selective

for the nickel(II) ion (*31*). In the metalloregulatory proteins Fur and Zur, a high affinity site binds a zinc(II) ion that is proposed to play a largely structural role and a lower affinity site is proposed to be the selective sensory site for iron(II) and zinc(II), respectively (*32*−*34*). In DtxR, the primary site (Figure 2, site A) is proposed to be a structural/ancillary site, while the secondary site (Figure 2, site B) is required for DNA binding activity (*10*). In contrast, MntR may have fused the functions of both a quintessential structural and a sensory site by having a single binuclear site. More extensive mutagenesis, structural, and biophysical studies will be necessary to elucidate all of the structural dynamics and metal site requirements for MntR activation.

ACKNOWLEDGMENT

We thank Dr. Emmanuel Guedon (Helmann Lab, Cornell University) for providing the protein vectors, Prof. Elizabeth Komives (U.C. San Diego) for assistance with use of the analytical ultracentrifuge and MALDI-TOF mass spectrometer, Prof. Patricia A. Jennings for assistance with the CD measurements and many helpful discussions, and Dr. Kevin Walda, Dr. Annette Deyhle, and Christopher Mahn (Scripps Institute of Oceanography) for access and assistance with the ICP-OES.

SUPPORTING INFORMATION AVAILABLE

Figures S1−S6 containing CD spectra, ultracentrifugation data, thermal denaturation curves, and fluorescence anisotropy data. This material is available free of charge via the Internet at http://pubs.acs.org.

REFERENCES

1. Outten, F. W., Outten, C. E., and O'Halloran, T. V. (2000) in *Bacterial stress responses* (Storz, G., and Hengee-Aronis, R., Eds.) pp 145−157, ASM Press, Washington, DC.
2. O'Halloran, T. V. (1993) Transition metals in control of gene expression, *Science 261*, 715−725.
3. Busenlehner, L. S., Pennella, M. A., and Giedroc, D. P. (2003) The SmtB/ArsR family of metalloregulatory transcriptional repressors: structural insights into prokaryotic metal resistance, *FEMS Microbiol. Rev. 27*, 131−143.
4. Que, Q., and Helmann, J. D. (2000) Manganese homeostasis in *Bacillus subtilis* is regulated by MntR, a bifunctional regulator related to the diphtheria toxin repressor family of proteins, *Mol. Microbiol. 35*, 1454−1468.
5. Guedon, E., and Helmann, J. D. (2003) Origins of metal ion selectivity in the DtxR/MntR family of metalloregulators, *Mol. Microbiol. 48*, 495−506.
6. Lieser, S. A., Davis, T. C., Helmann, J. D., and Cohen, S. M. (2003) DNA-binding and oligomerization studies of the manganese(II) metalloregulatory protein MntR from *Bacillus subtilis*, *Biochemistry 42*, 12634−12642.
7. Guedon, E., Moore, C. M., Que, Q., Wang, T., Ye, R. W., and Helmann, J. D. (2003) The global transcriptional response of *Bacillus subtilis* to manganese involves the MntR, Fur, TnrA and σ^B regulons, *Mol. Microbiol. 49*, 1477−1491.
8. Schmitt, M. P., Twiddy, E. M., and Holmes, R. K. (1992) Purification and characterization of the diphtheria toxin repressor, *Proc. Natl. Acad. Sci. U.S.A. 89*, 7576−7580.
9. Tao, X., Schiering, N., Zeng, H.-Y., Ringe, D., and Murphy, J. R. (1994) Iron, DtxR, and the regulation of diphtheria toxin expression, *Mol. Microbiol. 14*, 191−197.
10. Spiering, M. M., Ringe, D., Murphy, J. R., and Marletta, M. A. (2003) Metal stoichiometry and functional studies of the diphtheria toxin repressor, *Proc. Natl. Acad. Sci. U.S.A. 100*, 3808−3813.
11. Posey, J. E., Hardham, J. M., Norris, S. J., and Gherardini, F. C. (1999) Characterization of a manganese-dependent regulatory protein, TroR, from *Treponema pallidum*, *Proc. Natl. Acad. Sci. U.S.A. 96*, 10887−10892.
12. Jakubovics, N. S., Smith, A. W., and Jenkinson, H. F. (2000) Expression of the virulence-related Sca (Mn^{2+}) permease in *Streptococcus gordonii* is regulated by a diphtheria toxin metallorepressor-like protein ScaR, *Mol. Microbiol. 38*, 140−153.
13. Hill, P. J., Cockayne, A., Landers, P., Morrissey, J. A., Sims, C. M., and Williams, P. (1998) SirR, a novel iron-dependent repressor in *Staphylococcus epidermidis*, *Infect. Immun. 66*, 4123−4129.
14. Hazlett, K. R. O., Rusnak, F., Kehres, D. G., Bearden, S. W., La Vake, C. J., La Vake, M. E., Maguire, M. E., Perry, R. D., and Radolf, J. D. (2003) The *Treponema pallidum tro* operon encodes a multiple metal transporter, a zinc-dependent transcriptional repressor, and a semi-autonomously expressed phosphoglycerate mutase, *J. Biol. Chem. 278*, 20687−20694.
15. Glasfeld, A., Guedon, E., Helmann, J. D., and Brennan, R. G. (2003) Structure of the manganese-bound manganese transport regulator of Bacillus subtilis, *Nat. Struct. Biol. 10*, 652−657.
16. Pohl, E., Holmes, R. K., and Hol, W. G. J. (1999) Crystal structure of the iron-dependent regulator (IdeR) from *Mycobacterium tuberculosis* shows both metal binding sites fully occupied, *J. Mol. Biol. 285*, 1145−1156.
17. Pohl, E., Holmes, R. K., and Hol, W. G. J. (1999) Crystal structure of a cobalt-activated diphtheria toxin repressor-DNA complex reveals a metal-binding SH3-like domain, *J. Mol. Biol. 292*, 653−667.
18. White, A., Ding, X., vanderSpek, J. C., Murphy, J. R., and Ringe, D. (1998) Structure of the metal-ion-activated diphtheria toxin repressor/*tox* operator complex, *Nature 394*, 502−506.
19. Pace, C. N., Vajdos, F., Fee, L., Grimsley, G., and Gray, T. (1995) How to measure and predict the molar absorption coefficient of a protein, *Protein Sci. 4*, 2411−2423.
20. VanZile, M. L., Cosper, N. J., Scott, R. A., and Giedroc, D. P. (2000) The zinc metalloregulatory protein *Synechococcus* PCC7942 SmtB binds a single zinc ion per monomer with high affinity in a tetrahedral coordination geometry, *Biochemistry 39*, 11818−11829.
21. Melo, E. P., Faria, T. Q., Martins, L. O., Gonçalves, A. M., and Cabral, J. M. S. (2001) Cutinase unfolding and stabilization by trehalose and mannosylglycerate, *Proteins 42*, 542−552.
22. Ghadiri, M. R., and Choi, C. (1990) Secondary structure nucleation in peptides. Transition metal ion stabilized α-helices, *J. Am. Chem. Soc. 112*, 1630−1632.
23. Wang, S. C., Dias, A. V., Bloom, S. L., and Zamble, D. B. (2004) Selectivity of metal binding and metal-induced stability of *Escherichia coli* NikR, *Biochemistry 43*, 10018−10028.
24. Uversky, V. N., Winter, S., and Löber, G. (1998) Self-association of 8-anilino-1-naphthalene-sulfonate molecules: spectroscopic characterization and application to the investigation of protein folding, *Biochim. Biophys. Acta 1388*, 133−142.
25. Twigg, P. D., Parthasarathy, G., Guerrero, L., Logan, T. M., and Caspar, D. L. D. (2001) Disordered to ordered folding in the regulation of diphtheria toxin repressor activity, *Proc. Natl. Acad. Sci. U.S.A. 98*, 11259−11264.
26. Lakowicz, J. R. (1999) *Principles of fluorescence spectroscopy*, Kluwer Academic/Plenum Publishers, New York.
27. Eicken, C., Pennella, M. A., Chen, X., Koshlap, K. M., VanZile, M. L., Sacchettini, J. C., and Giedroc, D. P. (2003) A metal-ligand-mediated intersubunit allosteric switch in related SmtB/ArsR zinc sensor proteins, *J. Mol. Biol. 333*, 683−695.
28. Kuwajima, K., and Arai, M. (2000) in *Mechanisms of protein folding* (Pain, R. H., Ed.) pp 139−174, Oxford University Press, Oxford.
29. Pohl, E., Holmes, R. K., and Hol, W. G. J. (1998) Motion of the DNA-binding domain with respect to the core of the diphtheria toxin repressor (DtxR) revealed in the crystal structures of apo- and holo-DtxR, *J. Biol. Chem. 273*, 22420−22427.
30. Chen, C. S., White, A., Love, J., Murphy, J. R., and Ringe, D. (2000) Methyl groups of thymine bases are important for nucleic acid recognition by DtxR, *Biochemistry 39*, 10397−10407.
31. Bloom, S. L., and Zamble, D. B. (2004) Metal-selective DNA-binding response of *Escherichia coli* NikR, *Biochemistry 43*, 10029−10038.
32. Pohl, E., Haller, J. C., Mijovilovich, A., Meyer-Klaucke, W., Garman, E., and Vasil, M. L. (2003) Architecture of a protein central to iron homeostasis: crystal structure and spectroscopic analysis of the ferric uptake regulator, *Mol. Microbiol. 47*, 903−915.
33. Althaus, E. W., Outten, C. E., Olson, K. E., Cao, H., and O'Halloran, T. V. (1999) The ferric uptake regulator (Fur) repressor is a zinc metalloprotein, *Biochemistry 38*, 6559−6569.
34. Outten, C. E., Tobin, D. A., Penner-Hahn, J. E., and O'Halloran, T. V. (2001) Characterization of the metal receptor sites in *Escherichia coli* Zur, an ultrasensitive zinc(II) metalloregulatory protein, *Biochemistry 40*, 10417−10423.

BI0480741